5. M. E. Britton, in *Arctic Biology*, P. Hansen, Ed. (Oregon State Univ. Press, Corvallis, 1967), pp. 67–130.
6. D. M. Troy *et al.*, in *Prudhoe Bay Waterfowl Environmental Monitoring Program 1982* (report prepared for U.S. Army Corps of Engineers, Alaska District, Anchorage, AK, 1983).
7. A. L. Washburn, *Geocryology, a Survey of Periglacial Processes and Environments* (Wiley, New York, 1980).
8. P. J. Webber and J. D. Ives, *Environ. Conserv.* **5**, 171 (1978).
9. D. E. Lawson, *Arct. Alp. Res.* **18**, 1 (1986).
10. L. F. Klinger *et al.*, in *Proceedings of the Fourth International Permafrost Conference*, Fairbanks, AK, 1983, pp. 628–633.
11. D. A. Walker and K. R. Everett, *Arct. Alp. Res.*, in press.
12. D. Strayer *et al.*, "Long-term ecological studies: An illustrated account of their design, operation, and importance to ecology," *Occas. Publ. Inst. Ecosystem Stud.* **2** (1986).
13. J. G. Gosselink and L. C. Lee, "Cumulative impact assessment in bottomland hardwood forests" (LSU-CEI-86-09, Center for Wetland Resources, Louisiana State University, Baton Rouge, 1987).
14. R. F. Noss and L. D. Harris, *Environ. Manage.* **10**, 299 (1986).
15. G. E. Beanlands *et al.*, "Cumulative environmental effects: A binational perspective" (Canadian Environmental Assessment Research Council, Ottawa, Ontario, and National Research Council, Washington, DC, 1987).
16. L. D. Harris, *The Fragmented Forest* (Univ. of Chicago Press, Chicago, 1984).
17. G. C. Horak *et al.*, "Methodological guidance for assessing cumulative impacts on fish and wildlife" (U.S. Fish and Wildlife, Eastern Energy and Land Use Team, Kearneysville, WV, 1983).
18. P. Adamus and L. R. Stockwell, "A method for wetland functional assessment" (Federal Highway Administration, Washington, DC, 1983), vol. 1, FHWA-IP-82-23; vol. 2, FHWA-IP-82-24.
19. D. A. Walker *et al.*, *Environ. Conserv.* **13**, 149 (1986). Geobotanical and anthropogenic disturbance maps were produced at 1:6000 scale from the Prudhoe Bay Oil Field GIS database which consists of 19 components: 10 geobotanical variables, 3 years of natural disturbance information, and 6 years of anthropogenic disturbance. This information has been integrated into a single composite map called an Integrated Geobotanical and Historical Disturbance Map. Maps of any single variable or maps based on models involving numerous variables are produced from the database using the ARC/INFO GIS software. The database is useful for testing hypotheses involving landscape-anthropogenic disturbance interactions. The maps were used to examine the details of disturbance within three intensive study areas (Fig. 1) in the most heavily disturbed portions of the oil field. A 1:24,000 scale map was made to determine the full extent of roads, gravel-covered tundra, and large impoundments (Fig. 4).
20. D. A. Walker *et al.*, "Cumulative landscape impacts in the Prudhoe Bay Oil Field 1949–1983" (report prepared for U.S. Fish and Wildlife Service, Habitat Resources Section, Anchorage, AK, 1986).
21. K. R. Everett *et al.*, in *Proceedings of the Third International Conference on Permafrost* (National Research Council of Canada, Ottawa, 1978), pp. 359–365.
22. D. A. Walker *et al.*, *Geobotanical Atlas of the Prudhoe Bay Region, Alaska* (Report 80-14, U.S. Army Cold Regions Research and Engineering Laboratory, Hanover, NH, 1985).
23. D. A. Walker, *Vegetation and Environmental Gradients of the Prudhoe Bay Region, Alaska* (Report 85-14, U.S. Army Cold Regions Research and Engineering Laboratory, Hanover, NH, 1985).
24. _____ and W. Acevedo, *Vegetation and a Landsat-Derived Land Cover Map of the Beechey Point Quadrangle, Arctic Coastal Plain, Alaska* (Report 87-5, U.S. Army Cold Regions Research and Engineering Laboratory, Hanover, NH, 1987).
25. D. A. Walker *et al.*, *Landsat-Assisted Environmental Mapping in the Arctic National Wildlife Refuge, Alaska* (Report 82-87, U.S. Army Cold Regions Research and Engineering Laboratory, Hanover, NH, 1982).
26. D. A. Walker *et al.*, *Arct. Alp. Res.* **17**, 321 (1985).
27. M. D. Walker, thesis, University of Colorado, Boulder, CO (1987).
28. A. Lachenbruch and B. V. Marshall, *Science* **234**, 689 (1986).
29. R. T. T. Forman and M. Godron, *Landscape Ecology* (Wiley, New York, 1986).
30. Funded by the U.S. Environmental Protection Agency and the Cold Climate Environmental Research Program under U.S. Department of Energy Interagency Agreement DE-A-106-84RL10584 with the U.S. Fish and Wildlife Service, Habitat Resources Section, Anchorage, AK. Support for manuscript preparation came from the DOE Response, Resistance, Resilience and Recovery from Disturbance to Arctic Ecosystems (R4D) program. We thank the North Slope Borough, the Environmental Systems Research Institute, Inc., Sohio Alaska Petroleum Co., and Arco Oil and Gas Co. for logistical support, funding, and help during these mapping programs. We thank R. Meehan for help in obtaining data and for providing helpful suggestions; J. Nickles, K. Bayha, T. Rockwell, R. Sumner, J. McCarty, J. States, and J. Brown for sponsoring and encouraging this work.

Millisecond Pulsar PSR 1937+21: A Highly Stable Clock

L. A. Rawley,* J. H. Taylor,† M. M. Davis, D. W. Allan

The stable rotation and sharp radio pulses of PSR 1937+21 make this pulsar a clock whose long-term frequency stability approaches and may exceed that of the best atomic clocks. Improvements in measurement techniques now permit pulse arrival times to be determined in 1 hour at the Arecibo radio telescope with uncertainties of about 300 nanoseconds relative to atomic time. Measurements taken approximately every 2 weeks since November 1982 yield estimates of fractional frequency stability that continue to improve with increasing averaging time. The pulsar's frequency stability is at least as good as 6×10^{-14} for averaging times longer than 4 months, and over the longest intervals the measurements appear to be limited by the stability of the reference atomic clocks. The data yield a firm upper limit of 7×10^{-36} gram per cubic centimeter for the energy density of a cosmic background of gravitational radiation at frequencies of about 0.23 cycle per year. This limit corresponds to approximately 4×10^{-7} of the density required to close the universe.

A RAPIDLY SPINNING NEUTRON STAR, BRAKED ONLY BY THE magnetic dipole radiation that gives rise to its beamed radio emission, is a potential frequency standard free from the perturbations of the solar system (*1*). Despite their impressive stabilities (*2*), the moderate rotation frequencies (ν) of most pulsars (0.5 to 5 Hz) limit the precision of timing measurements to $\gtrsim 100$ μsec, about an order of magnitude less than the precision of modern cesium clocks on time scales of a few years. Furthermore, most pulsars are young objects, no more than a few million years old; their magnetic moments are apparently decaying, and the neutron stars are still cooling and stabilizing after the catastrophic supernova explosions in which they were formed. Consequently, these "ordinary" pulsars exhibit low-level frequency instabilities $\Delta\nu/\nu \gtrsim 10^{-12}$ over time scales longer than a few years (*3*).

L. A. Rawley and J. H. Taylor are in the Physics Department, Princeton University, Princeton, NJ 08544. M. M. Davis is at the Arecibo Observatory, Arecibo, PR 00613. D. W. Allan is at the Time and Frequency Division, National Bureau of Standards, Boulder, CO 80303.

*Present address: Applied Research Corporation, Landover, MD 20785.
†To whom correspondence should be sent.

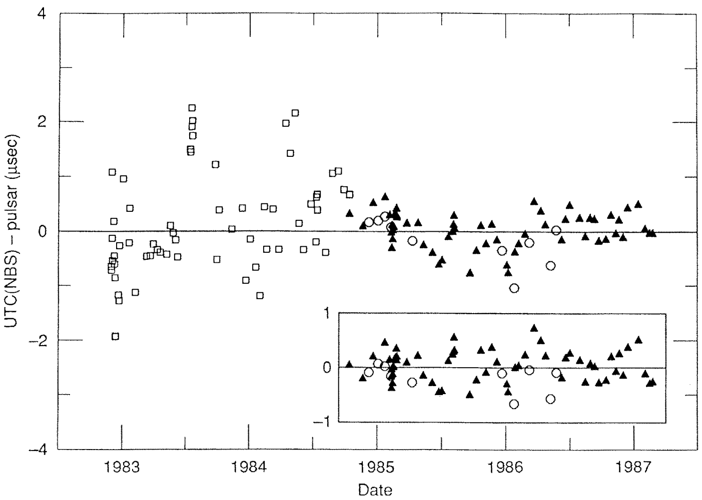

Fig. 1. Post-fit arrival-time residuals for PSR 1937+21. Open squares represent 1408-MHz data, referred to UTC(NBS) by means of LORAN-C and corrected for the fixed dispersion constant listed in Table 1. Filled triangles represent data taken at 2380 MHz, or at both 1408 and 2380 MHz on the same day, referred to UTC(NBS) by means of the GPS satellite observations and corrected for a smoothed 70-day mean dispersion measure [see text and (*5*)]. Open circles are based on 1408-MHz data alone, but are otherwise similar to the triangles. The inset shows residuals from a fit to the data acquired since October 1984, and gives the best indication of the accuracy of the most recent observations.

The discovery (*4*) of millisecond pulsars—especially PSR 1937+21, the fastest and strongest of the four now known—has renewed interest in the applications of high precision pulsar timing observations. In another article (*5*) we have discussed some interesting astrometric and astrophysical applications of 4.2 years of timing observations of this object. Here we concentrate on two other applications of the same set of measurements: comparisons of the stabilities of "pulsar time" and atomic time, and the determination of a new upper limit to a cosmic background of gravitational radiation (*6*).

The possibility of studying long-term effects of order $\lesssim 1$ μsec took pulsar observers by surprise: the equipment with which the initial timing data (*7*) on PSR 1937+21 were taken was designed under the assumption that systematic errors of this size could safely be ignored. In this article we describe recent results obtained with new equipment in which many instrumental deficiencies have been corrected, and we present a detailed analysis of all results obtained since late 1982.

Observations

Timing observations of PSR 1937+21 have been made with the Arecibo Observatory's 305-m telescope at intervals of 2 to 3 weeks, and occasionally more frequently, starting in November 1982. Results from the first 2 years of data have already been published (*7*); briefly, those data consist of 62 single-day arrival time measurements made at a frequency of 1408 MHz, with typical uncertainties of a little less than 1 μsec. In October 1984 a new data acquisition system was installed (*8*). With the new system, signals of both left and right circular polarization are received at radio frequencies of 1408 or 2380 MHz, amplified, and detected in a 2 by 32 channel filter-bank spectrometer with 0.25-MHz channel width. The output of each filter channel, summed over polarizations, is sampled at 128 times the expected pulsar frequency by one of 32 synchronously operating signal averagers. In this way the pulsar's periodic waveform is accumulated into 32 integrated pulse profiles, each with 128 equally spaced phase bins. The profiles are saved in digital form every 2 minutes, together with a fiducial time recorded from the observatory's master clock at a specified phase in the signal averager cycle. The recorded profiles are analyzed by template matching in the Fourier transform domain to determine pulse phases (*8*). The phases (in cycles) are multiplied by the pulse period and added to the fiducial times to produce topocentric arrival times for the main stage of data analysis.

This procedure incorporates three improvements over that used during the 1982–1984 observations. Two of the improvements are related to dispersion of the pulsar signals in the partially ionized interstellar medium, which at observing frequency $f_{\rm obs}$ causes an excess propagation delay $\delta T_D(f) = D/f^2_{\rm obs}$. [Here D is the "dispersion constant" of the pulsar, proportional to the integral of free-electron density along the line of sight; see (*9*) for additional details.] By observing for about 1 hour at each of our two frequencies on each observing day, we can monitor changes in D at the level of 1 part in 10^5, and thereby avoid confusing its small variations with other sources of timing noise. Second, we have chosen to record the data from each filter channel separately, and remove the dispersive time offsets among channels in data analysis, instead of summing the filter outputs along a dispersion-compensating digital delay line as was done previously (*10*). The linear approximation to $\delta T_D(f)$ used by the hardware de-disperser is inaccurate by as much as 1.5 μsec over the 8-MHz total bandwidth, and intensity variations across the passband induced by diffractive interstellar scintillation (*4, 5*) have time and frequency scales such that the summed signal sometimes bears the full effect of the nonlinearity. Finally, we reference the observatory's clock to atomic time via the Global Positioning System (GPS) satellites instead of relying on LORAN-C timing signals, which are subject to small but significant diurnal and annual variations in propagation delay.

Arrival Time Analysis

In the rest frame of a well-behaved neutron star, its rotation phase ϕ is closely approximated by the simple expression

$$\phi(t) = \phi_0 + \nu_0 t + \frac{1}{2}\dot{\nu}t^2 \qquad (1)$$

where ϕ_0 is the phase in cycles at some reference time $t = 0$, and ν_0 and $\dot{\nu}$ are the rotation frequency and its first derivative. The proper time t in the pulsar's reference frame is related to the terrestrial atomic time of the ith observation, T_i, by the transformation

$$t(T_i) = T_i - |\mathbf{d} - \mathbf{r}|/c - \delta T_D - \delta T_C - \delta T_R \qquad (2)$$

Here $\mathbf{d}$ is the vector from the solar system barycenter (SSBC) to the pulsar, r is the vector from the SSBC to the observing site, δT_D is the dispersion delay defined earlier, δT_C is the correction from the observatory's master clock to some realization of proper atomic time on the earth, and δT_R incorporates relativistic terms resulting from the motions of the earth and the varying total gravitational potential at the clock. Uncertainty in the magnitude of $\mathbf{d}$ is harmlessly absorbed into the definition of ϕ_0; similarly, lack of knowledge of the pulsar's radial velocity causes a small and uninteresting bias in the derived value of ν_0.

In practice we determine the clock correction δT_C by measuring the time offset between the observatory master clock and a local cesium standard at the time of observation. To this we add an additional correction for the offset of the cesium clock relative to UTC(NBS)—the version of Coordinated Universal Time maintained and distributed by the U.S. National Bureau of Standards. This correction is determined by measurements made through the

GPS satellites. The error in time transfer with this technique, including the effects of uncorrected drifts in the various oscillators and phase noise in the necessary comparisons, is believed to be less than 30 nsec.

We have described the procedure used to determine the dispersive delays δT_D elsewhere (*5*). Briefly, the pulse arrival times at two frequencies are used to determine a correction δD to the dispersion "constant" D for each observing day. A smoothed approximation to these numbers is obtained by computing a running mean (with Gaussian weighting, 70 days full width at half maximum). The smoothed values are added to D before performing the time transformation of Eq. 2. Since October 1984 the measured interstellar dispersion has exhibited a random-walk behavior with maximum peak-to-peak excursion $\delta D/D = 2.3 \times 10^{-5}$, corresponding to differential delays of up to ± 1.1 μsec between our two observing frequencies. We estimate that in these data timing errors introduced by imperfect dispersion corrections could amount to as much as 70 nsec at 2380 MHz and 200 nsec at 1408 MHz. In the 1982–1984 data, when dispersion changes were not being monitored, errors from this cause could be as large as 1 μsec.

The complexity of the solar system requires that computation of $\mathbf{r}(T_i)$ and $\delta T_R(T_i)$ be done with a highly accurate ephemeris of the earth's motion. We currently use the PEP740R ephemeris, produced and maintained at the Harvard–Smithsonian Center for Astrophysics (*11*). This ephemeris, based on numerical integration of a model solar system whose parameters are determined from planetary radar and spacecraft ranging measurements in the inner solar system, is believed to contribute errors in our analysis no larger than ~100 nsec over time intervals up to a year or so. Over longer spans its accuracy is less well known but is certainly not as good. Ephemeris errors could begin to affect our analysis at present levels of accuracy after intervals of several years or longer.

The main phase of data analysis is carried out by performing the transformation of Eq. 2 for each measured pulse arrival time; we then use a linearized least-squares method to compute small corrections to model parameters, minimizing the sum of squared deviations of $\phi[t(T_i)]$ from integer values. The correct pulse numbering is completely unambiguous, even after gaps in the data as large as 10^9 pulse periods. In fact, if present levels of stability are maintained, gaps of 20 years or more ($>4 \times 10^{11}$ periods) could be accommodated without loss of correct pulse numbering.

The principal free parameters in the model are the pulsar's initial phase ϕ_0, frequency ν_0, frequency derivative $\dot{\nu}$, and two celestial coordinates that specify the direction of $\mathbf{d}$. Together with the dispersion constant D, these five parameters are sufficient to specify the timing behavior of PSR 1937+21 to ~2-μsec accuracy over a few years. The post-fit residuals are reduced still further—to a root-mean-square (rms) magnitude of approximately 0.3 μsec in the data since October 1984—by including two additional free parameters, the first time derivatives of the celestial coordinates of the pulsar.

Post-fit residuals for two solutions to the data through 24 February 1987 are illustrated in Fig. 1. The principal solution, which yielded the parameters listed in Table 1, includes the full 4.2 years of data. The data for July 1983 and April–May 1984, which appear to be flawed, were given zero weight in this solution; they are included in Fig. 1 as indicators of the largest systematic errors (of unknown cause) present in the early data. The weighted rms deviation of the remaining residuals in the 1982–1984 data is 580 nsec. The inset to Fig. 1 shows residuals from a fit to the data since October 1984. In this solution a small increase in estimated period derivative, approximately 1.4 times the uncertainty quoted in Table 1, has removed the upward curvature evident in the residuals from the full solution over the same time span. For the 1984–1987 data the rms residual is 301 nsec.

Comparison of Clock Stabilities

Careful inspection of Fig. 1 reveals that, even apart from the questionable measurements made in July 1983 and April–May 1984, the post-fit residuals do not have the character of zero-mean Gaussian noise. The largest contributions to systematic errors in the 1982–1984 data are believed to come from instrumental limitations in correcting for interstellar dispersion (*8*), unmeasured variations in the total electron content along the line of sight, and errors in time transfer by means of LORAN-C. Squinting obliquely along the long axis of Fig. 1 helps one to see another systematic trend, a quasi-cubic behavior that starts low and ends high, with a local maximum near 1984.0 and a minimum near 1986.0. It is extremely unlikely that these trends are the result of the secular braking process acting on the pulsar; on the contrary, such behavior is exactly the kind expected when a stochastic process containing excess low-frequency noise is analyzed by subtracting a fitted polynomial such as that in Eq. 1. The resulting residuals usually show a trend corresponding to the first omitted term in the polynomial, in this case the cubic term.

The dimensionless stability of a clock and its spectral dependence can be meaningfully characterized in terms of the modified Allan variance, $\tilde{\sigma}_y^2(\tau)$, measured over various time intervals τ. Note that our procedure of fitting an astrophysical model to measurements of pulsar time minus atomic time necessarily absorbs some fraction of the differences into biases in the fitted parameters. Consequences of this have been explored at length elsewhere (*6*); these authors derive a transmission coefficient $T(f)$ that specifies the fraction of timing noise power remaining in the residuals at fluctuation frequency f after the astrophysical parameters have been extracted. Using this approach, we compute modified Allan variances from the pulsar residuals according to the relation

$$\tilde{\sigma}_y^2(\tau) = \frac{1}{2\mathcal{g}(\tau)}\left\langle\left[\frac{\bar{R}(t+\tau) - 2\bar{R}(t) + \bar{R}(t-\tau)}{\tau}\right]^2\right\rangle \qquad (3)$$

where $\bar{R}(t)$ is the average of all residuals obtained at times between $t - \tau/2$ and $t + \tau/2$, the angled brackets signify an average taken over all available triplets of averaging intervals spaced by $\pm\tau$, and $\mathcal{g}(\tau)$ is an average of the transmission coefficient $T(f)$ over an octave frequency range centered at $f = 1/2\tau$. For our data, $\mathcal{g}(\tau) \approx 1.0$ for time scales $\tau < 10^7$ seconds. At $\tau = 2.2 \times 10^7$ seconds = 256 days, the longest time scale for which reasonable statistics are available, $\mathcal{g} = 0.66$.

Computed values of $\tilde{\sigma}_y(\tau)$ for our measurements of PSR

Table 1. Measured parameters of PSR 1937+21. Quoted uncertainties for all parameters are three to eight times the formal standard errors from the least-squares fitting procedure, and include our best estimates of the magnitude of possible systematic errors. The uncertainty in period refers to the last digit quoted. Our unit of time is the SI second as approximated by UTC(NBS) during the period 1982.9–1987.1, and celestial coordinates and proper motion are based on the reference frame of the Center for Astrophysics PEP740R ephemeris. Note that the accuracies specified for both period and position exceed the degree of agreement between measurement standards. In general, the uncertainties include allowance for plausible systematic errors in the data (*5*), but not for errors in the reference standards relative to their definitions.

Period (msec)	1.55780644887275 ± 3
Period derivative (10^{-20} sec sec^{-1})	10.51054 ± 0.00008
Right ascension (1950.0)	$19^h37^m28^s.74601 \pm 0.00002$
Declination (1950.0)	21°28′01″.4588 ± 0.0003
Epoch (Julian ephemeris date)	2445303.2940
Proper motion in right ascension (year^{-1})	−0″.0003 ± 0″.0002
Proper motion in declination (year^{-1})	−0″.0005 ± 0″.0003
Dispersion constant (10^{16} sec^{-1})	29.479 ± 0.001

Fig. 2. Fractional frequency stabilities $\bar{\sigma}_y(\tau)$ for measurements of PSR 1937+21 relative to UTC(NBS) (filled circles) and UTC(NBS) relative to other atomic time standards (open circles). Error bars correspond to standard deviations of the means of available estimates for each plotted point. The dashed line represents a model of the stability of UTC(NBS); the solid line is the locus of $\bar{\sigma}_y(\tau)$ values that would be observed for a perfect clock measured once every 16 days with 300-nsec random measurement errors (white phase noise).

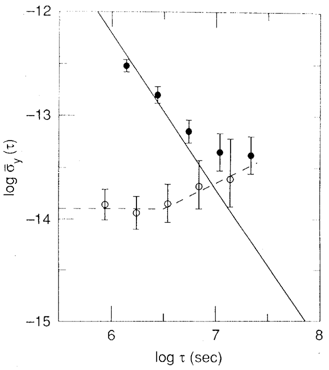

1937+21 are plotted as filled circles in Fig. 2. Values for $\tau \leq 1.1 \times 10^7$ seconds (128 days) are based on the higher quality 1984–1987 data alone; the last point, for $\tau = 2.2 \times 10^7$ seconds = 256 days, is based on the full 4.2-year data set. For comparison purposes, Fig. 2 also includes estimates of the stability of the reference time scale UTC(NBS) over the period 1984.4–1987.1 (open circles). We obtained these estimates by monitoring UTC(NBS) relative to a weighted set of the data from other principal timing centers around the world. Dashed line segments drawn through the open circles constitute a plausible model of the stability of UTC(NBS) (*12*). Figure 2 also includes a solid line corresponding to the $\bar{\sigma}_y(\tau)$ values that would be measured for a perfect clock contaminated by 300 nsec of uncorrelated measurement errors or "white phase noise," with an average sampling interval of 16 days.

Over time intervals $\tau < 3 \times 10^6$ seconds (about 1 month), the estimates of $\bar{\sigma}_y(\tau)$ for PSR 1937+21 are dominated by uncertainties in measuring the phase of the pulsar waveform. Most of this uncertainty appears to be random, and although we are aware of ways in which the measurement procedure at the radio telescope and the data analysis could still be improved, these sources do not presently impose accuracy limitations at the 300-nsec level. For time scales of 2 to 4 months, Fig. 2 shows marginal evidence of instability in excess of that attributable to the reference time standard. We believe this most likely results from errors in the corrections for variable interstellar dispersion (*5*), or possibly from small changes in effective path length to the pulsar caused by refractive effects in the interstellar medium (*13*). Further observations, preferably at higher radio frequencies, will be required to test these conjectures.

Over time scales exceeding about 6 months, Fig. 2 suggests strongly that observations of PSR 1937+21 at Arecibo have been limited by the stability of existing atomic time and frequency standards. In particular, the measured value of $\bar{\sigma}_y(\tau)$ for τ = 256 days falls nearly on the extrapolated stability curve for UTC(NBS); since it cannot be expected to fall below this line, its position well above the line that shows 300-nsec white phase noise is no indication of instability inherent in the pulsar. It is likely, in fact, that all of the filled circles in Fig. 2 represent only upper limits to the true frequency stability of PSR 1937+21. For time intervals greater than about half a year, this pulsar could be the most stable time and frequency reference known.

UTC(NBS) is a "steered" time scale designed to stay within 1 μsec of UTC, the internationally coordinated version of atomic time. The National Bureau of Standards also maintains an unsteered, locally generated proper time scale called AT1, and we have also analyzed our measurements of PSR 1937+21 with respect to AT1. The results show that since late 1984, the pulsar timing residuals relative to AT1 are marginally smaller than those relative to UTC(NBS). Over the full 4.2 years, however, the pulsar data indicate that AT1 was less stable than UTC(NBS), mostly the result of a frequency change of slightly more than 2 parts in 10^{13} during the first half of 1984. Such a change, only twice the estimated uncertainty of the best primary frequency standards, is difficult to detect with certainty in direct comparisons between a small number of atomic clocks. However, comparison of AT1 with clocks at both the National Research Council of Canada and the Physikalisch-Technische Bundesanstalt in the Federal Republic of Germany confirms both the epoch and the magnitude of the frequency shift seen in AT1 relative to PSR 1937+21.

Gravitational Radiation in the Universe

According to some cosmological theories (*14*), the universe may contain a substantial energy density in the form of a stochastic background of gravitational waves, analogous to the known cosmic microwave background (*15*). The gravitational background could in principle be detected by means of pulsar timing observations, because a gravitational wave passing the pulsar during time of pulse emission, or passing the earth during reception, would cause changes in the rates of local clocks relative to distant clocks (*16*). In practice, the range of accessible gravitational wave periods extends from the minimum observing interval to the total time spanned by the observations.

If, by hypothesis, we ascribe all of the nonzero PSR 1937+21 timing residuals to this cause, we can obtain a firm upper limit to the energy density in gravitational waves over the relevant frequency interval. Such an exercise was already carried out for our 1982–1984 data (*7*), yielding the limit $\rho < 1 \times 10^{-32}$ g cm^{-3} for the equivalent density of gravitational radiation in the frequency range $1 < f < 3$ cycles per year. We can now improve substantially on this limit, for several reasons. With the baseline of data extended from 1.9 to 4.2 years, the minimum frequency to which we are sensitive has decreased proportionally, and the average transmission coefficients $\mathcal{J}(\tau)$ have increased. In addition, the more precise data obtained since October 1984 would allow lower limits to be set even over the same observing span. In order to make our results directly comparable with those previously published, we again use the procedure outlined in (*7*), and developed in detail in (*6*), to compute limits for $\rho(f)$. We obtain $\rho(f) < 1.7 \times 10^{-34}$ g cm^{-3} for $f \approx 0.8$ cycle per year, and $\rho(f) < 7 \times 10^{-36}$ g cm^{-3} for $f \approx 0.23$ cycle per year. In both cases the implied bandwidth is a factor of e, or slightly more than an octave, upward in frequency.

For a Hubble constant H_0 = 100 km sec^{-1} Mpc^{-1}, the critical density required to close the universe is $\rho_c = 3H_0^2/(8\pi G) = 2 \times 10^{-29}$ g cm^{-3}. Thus our limits correspond to fractions 9×10^{-6} and 4×10^{-7} of closure density, respectively. The latter figure is within a factor of 4 of the predicted radiation that would be produced by vibrating cosmic strings that may have been present in the early universe (*17*). Such strings have been postulated as an aid to galaxy formation; if they exist, then observations like those reported here should be able to detect their effects in just a few more years. Distinguishing a gravitational radiation background from instabilities in the pulsar, the reference clocks, or the propagation medium will be difficult, but not necessarily impossible—particularly if data are obtained from additional millisecond pulsars (*5*).

Conclusions

Timekeeping was for many years based on astronomical observations related to the rotation of the earth. In the last several decades, atomic clocks have been shown to be more stable than the rotation of the earth, and consequently the SI second was redefined (*18*). It now seems that another astronomical phenomenon—the rotation of a millisecond pulsar—may again rival the stability of the best available man-made clocks.

The technical challenge of pushing the precision of pulsar timing as far as possible is alluring to us as experimenters. And it appears likely that considerable further progress can be made. Present observations of PSR 1937+21 are limited not by telescope sensitivity, radiometer noise, or sky background temperature, but rather by systematic measurement errors that can still be reduced. Instrumental limitations of the radio frequency spectrometer are now being worked on. Observations at higher radio frequencies will almost certainly reduce the difficult-to-calibrate variations in propagation time through the interstellar medium, and will become feasible with high sensitivity if a proposed upgrading of the Arecibo telescope is carried out. At present we know of a second millisecond pulsar, PSR 1855+09, for which time-of-arrival measurements at the ~1 μsec level are already possible (*5*). More of these objects will likely be discovered in millisecond pulsar surveys now under way.

The evident need for a better time standard in this experiment is a strong motivation for builders and maintainers of atomic clocks. Steps are now in progress at NBS and at the Bureau International de l'Heure to combine the best clocks in the world in an optimum weighted algorithm to create the "world's best clock" as a reference. Atomic clocks have improved in stability by an order of magnitude every 7 years since their introduction in 1949, and we see no reason for this trend to stop in the near future (*19, 20*). We are also optimistic that more millisecond pulsars will be found, so that timing comparisons can be made among a number of them.

REFERENCES AND NOTES

1. B. Hoffmann, *Nature (London)* **218**, 667 (1968).
2. P. R. Backus, J. H. Taylor, M. Damashek, *Astrophys. J.* **215**, L63 (1982); G. S. Downs and P. Reichley, *Astrophys. J. Suppl.* **53**, 169 (1983).
3. J. M. Cordes and G. S. Downs, *Astrophys. J. Suppl.* **59**, 343 (1985); D. J. Helfand, J. H. Taylor, P. R. Backus, J. M. Cordes, *Astrophys. J.* **237**, 206 (1980).
4. D. C. Backer *et al.*, *Nature (London)* **300**, 615 (1982).
5. L. A. Rawley, J. H. Taylor, M. M. Davis, *Astrophys. J.*, in press.
6. R. Blandford, R. Narayan, R. W. Romani, *J. Astrophys. Astron.* **5**, 369 (1984).
7. M. M. Davis *et al.*, *Nature (London)* **315**, 547 (1985).
8. L. A. Rawley, thesis, Princeton University (1986).
9. R. N. Manchester and J. H. Taylor, *Pulsars* (Freeman, San Francisco, 1977), chap. 6.
10. V. Boriakoff, thesis, Cornell University (1973).
11. The PEP740R ephemeris and related software were kindly supplied by J. F. Chandler.
12. D. W. Allan and J. A. Barnes, *Proceedings of the 35th Annual Symposium on Frequency Control* (U.S. Army, Fort Monmouth, NJ, 1985), pp. 470–474.
13. R. Blandford and R. Narayan, in *Millisecond Pulsars*, S. P. Reynolds and D. R. Stinebring, Eds. (National Radio Astronomy Observatory, Green Bank, WV, 1984), p. 310.
14. For a review, see K. S. Thorne, in *Three Hundred Years of Gravitation*, S. W. Hawking and W. Israel, Eds. (Cambridge Univ. Press, Cambridge, in press).
15. D. T. Wilkinson, *Science* **232**, 1517 (1986).
16. S. Detweiler, *Astrophys. J.* **234**, 1100 (1979).
17. T. Vachaspati and A. Vilenkin, *Phys. Rev. D* **31**, 3052 (1985).
18. "The International System of Units (SI)," *NBS Special Publication 330* (U.S. Department of Commerce, Washington, DC, 1981).
19. D. W. Allan, *Proceedings of the 37th Annual Symposium on Frequency Control* (U.S. Army, Fort Monmouth, 1983), pp. 55–60.
20. D. J. Wineland, *Science* **226**, 395 (1984).

21. We thank A. Vázquez, R. Vélez, and A. S. Fruchter for data taking, J. Levine and T. Peppler for assistance in analysis, and D. R. Stinebring for many helpful discussions. This work was supported at Princeton by the National Science Foundation and was completed while J.H.T. was a Visiting Scientist at the Arecibo Observatory.

Molecular Genetics: Applications to the Clinical Neurosciences

Joseph B. Martin

Application of molecular biology, by means of linkage analysis and DNA probes that demonstrate restriction fragment length polymorphisms (RFLPs), has resulted in the chromosomal localization of the genes responsible for a number of neurological disorders. Characterization of the structure and function of individual genes for these diseases is in an early stage, but information available indicates that the molecular mechanisms underlying phenotypic expression of neurological diseases encompass a wide range of genetic errors ranging from the most minor (a single–base pair mutation) to large chromosomal deletions. Linkage analysis can now be used for genetic counseling in several of these disorders.

Until recently, the likelihood of discovering the molecular genetic basis of most neurological diseases seemed remote. Now, the application of molecular biology techniques, with DNA probes that reveal restriction fragment length polymorphisms (RFLPs) (*1*) combined with linkage analysis, has resulted in the chromosomal localization of the genes responsible for several of these disorders. In addition, more refined methods of cytogenetics have permitted recognition of chromosomal aberrations (deletions, translocations, or duplications) associated with some of these conditions (*2*). Furthermore, abnormal genes have now been cloned in some of the autosomal recessive lysosomal storage diseases. This review summarizes advances made in selected neurological disorders on which these recent discoveries have had a major impact (Table 1).

Genetic Linkage Analysis

DNA polymorphisms, first demonstrated in the β-globin gene family (*3*), have been used to identify the chromosomal location of the abnormal gene in Huntington's disease (*4*) (chromosome 4), Duchenne dystrophy (*5, 6*) (X chromosome), familial amyloidotic

The author is chief of the Neurology Service, Massachusetts General Hospital, and Julieanne Dorn Professor of Neurology, Harvard Medical School, Boston, MA 02114.